Available online at www.sciencedirect.com
ScienceDirect
Nuclear Physics B Proceedings Supplement – Preprint
Nuclear Physics B Proceedings Supplement

The NOvA experiment: status and outlook

R. B. Patterson[a,1]

[a] California Institute of Technology, Pasadena, California 91101

Abstract

The NOvA long-baseline neutrino oscillation experiment is currently under construction and will use an upgraded NuMI neutrino source at Fermilab and a 14-kton detector at Ash River, Minnesota to explore the neutrino sector. NOvA uses a highly active, finely segmented detector design that offers superb event identification capability, allowing precision measurements of $\nu_e/\overline{\nu}_e$ appearance and $\nu_\mu/\overline{\nu}_\mu$ disappearance, through which NOvA will provide constraints on θ_{13}, θ_{23}, $|\Delta m^2_{\text{atm}}|$, the neutrino mass hierarchy, and the CP-violating phase δ. In this article, we review NOvA's uniquely broad physics scope, including sensitivity updates in light of the latest knowledge of θ_{13}, and we discuss the experiment's construction and operation timeline.

Keywords: NOvA, neutrino, long-baseline, mixing, mass hierarchy, CP violation

1. Introduction

The NuMI Off-axis ν_e Appearance (NOvA) experiment is a two-detector, long-baseline, atmospheric-regime neutrino oscillation experiment designed to address a broad range of open questions in the neutrino sector through precision measurements of $\nu_\mu \to \nu_e$, $\overline{\nu}_\mu \to \overline{\nu}_e$, $\nu_\mu \to \nu_\mu$, and $\overline{\nu}_\mu \to \overline{\nu}_\mu$ oscillations. As the name implies, much of NOvA's physics scope comes from the appearance channels, as the observed rates of ν_e and $\overline{\nu}_e$ interactions provide information on (1) the ordering of the neutrino masses (*i.e.*, whether the ν_3 state is more or less massive than the other two), (2) the amount of CP violation present in the neutrino sector, (3) the size of the PMNS mixing angle θ_{13}, and (4) whether the ν_3 state has more ν_μ or ν_τ admixture (that is, whether $\theta_{23} > \frac{\pi}{4}$ or $< \frac{\pi}{4}$, respectively). Recent results by short-baseline $\overline{\nu}_e$ disappearance experiments demonstrating $\theta_{13} \approx 9^\circ$ [1, 2, 3] ensures that NOvA will have substantial event rates in the appearance channels. Through ν_μ and $\overline{\nu}_\mu$ disappearance, NOvA will provide improved precision on the dominant atmospheric oscillation parameters θ_{23} and $\left|\Delta m^2_{\text{atm}}\right|$.

Outside of these primary goals, NOvA will also look for evidence of new physics through comparisons of $\nu_\mu \to \nu_\mu$ and $\overline{\nu}_\mu \to \overline{\nu}_\mu$, provide constraints on sterile neutrino models by measuring the total flux of active neutrinos at its downstream detector, monitor for supernova neutrino activity, perform neutrino-nucleus cross section measurements with a narrow-band beam, and pursue a variety of non-neutrino topics including searches for magnetic monopoles and hidden sector particles.

For all of the oscillation measurements, NOvA takes advantage of a two-detector configuration to mitigate uncertainties in neutrino flux, neutrino cross sections, and event selection efficiencies. The 14-kton Far Detector (FD) is currently under construction in Ash River, Minnesota, 810 km downstream of the neutrino source at Fermilab. The 0.3-kton Near Detector (ND) will be located on the Fermilab site in a new cavern to be excavated near the existing MINOS Near Detector Hall.

2. Neutrino source

NOvA uses Fermilab's NuMI beamline as its neutrino source [4]. The NOvA detectors are situated 14 mrad off the NuMI beam axis, so they are exposed to a relatively narrow band of neutrino energies centered at 2 GeV.

[1] On behalf of the NOvA collaboration.

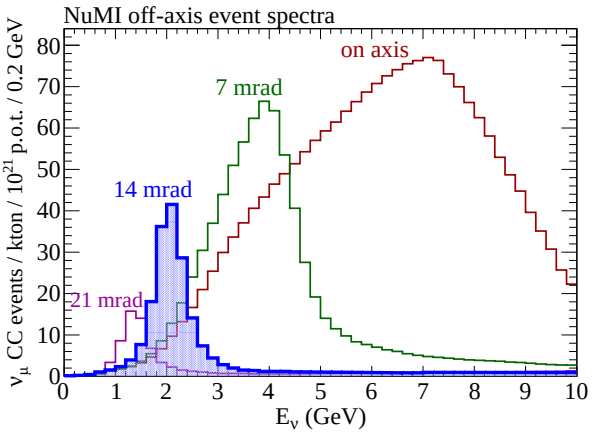

Figure 1: Simulated neutrino energy spectra for ν_μ charged current interactions in detectors sited 0, 7, 14, and 21 mrad off the NuMI beam axis. NOvA sits at 14 mrad.

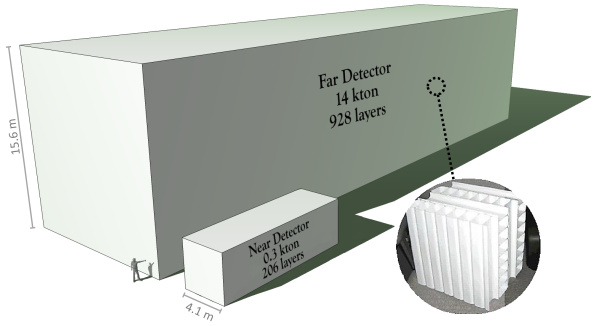

Figure 2: NOvA detectors, with a human figure shown for scale. The FD differs from the ND only in the length of its PVC cells and the number of layers present. Each layer in the detectors is oriented orthogonally to adjacent ones to provide 3D event reconstruction. (*Inset*) A cut-away view of the PVC cellular structure.

Figure 1 shows how the energy spectrum for ν_μ charged current (CC) events varies with detector position. The suppressed high-energy tail at NOvA's off-axis location reduces neutral current backgrounds in the visible energy range of 1 to 3 GeV where the appearance of ν_e CC events should occur.

The NuMI source is undergoing upgrades to increase its average beam power from 350 kW to 700 kW. Much of the increased power comes from a reduction in the Main Injector cycle time, which will drop from 2.2 seconds to 1.3 seconds. This cycle time reduction is in turn made possible by reconfiguring the antiproton Recycler as a proton injection ring, thereby allowing ramping in the Main Injector to occur concurrently with the next injection. The NuMI upgrades are scheduled to last 12 months, ending May 2013.

3. Detectors

The NOvA detectors are highly segmented, highly active tracking calorimeters. The segmentation and the overall mechanical structure of the detectors are provided by a lattice of PVC cells with cross sectional size (6 cm)×(4 cm). Each cell extends the full width or height of the detector – 15.6 m in the FD, 4.1 m in the ND – and is filled with liquid scintillator. Light produced by the scintillator is collected and transported to the end of the cell by a wavelength-shifting fiber that terminates on a pixel of a 32-channel avalanche photodiode. Figure 2 shows a sketch of the FD and ND along with a cut-away view of the PVC lattice. Each of the 928 layers of the FD has 384 cells, for ~360,000 total channels of readout. The ND has 206 layers each with 96 cells plus a muon range stack at the downstream end (not shown in the figure) made by interleaving steel plates with standard detector layers.

Figure 3 shows three simulated events in the NOvA ND. Muons are clearly identifiable as long, straight tracks with appropriate energy deposition per unit path-length ($\frac{dE}{dx}$). Proton tracks can be separated from other hadron tracks by their $\frac{dE}{dx}$ profiles. The NOvA detector technology is particularly well-suited for electromagnetic shower identification, as the radiation length in the detector (38 cm) is many times larger than the relevant PVC cell dimensions. This level of granularity helps π^0 decays stand out, as the decay photons leave telltale gaps in detector activity between the neutrino interaction location and the photon conversion point, as in the bottom panel of Figure 3.

Since November 2010, NOvA has operated a prototype detector, dubbed the Near Detector on the Surface (NDOS), that has allowed full-scale detector assembly and integration tests, electronics and data acquisition development, calibration R&D, Monte Carlo simulation tuning, and early analysis R&D. The NDOS sits 110 mrad off the NuMI beam axis and approximately on the Booster beam axis and is identical in size to the ND except in its width, with 64 cells spanning it horizontally rather than 96. With the NDOS, NOvA has recorded hundreds of neutrino interactions from both the NuMI and Booster sources and has collected millions of cosmic ray interactions. Figure 4 shows two distributions

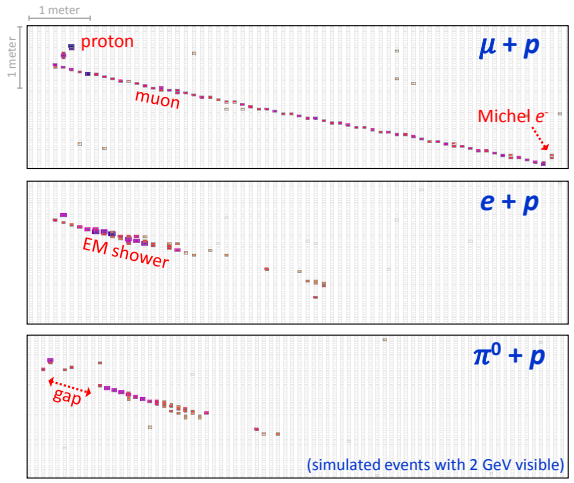

Figure 3: Simulated ND events with 2 GeV visible energy. Each colored rectangle corresponds to a single detector cell, with darker colors representing higher measured energy deposition. Only one of the two orthogonal detector views is shown for each event. (*Top*) ν_μ CC quasi-elastic event, with a muon and proton in the final state. The muon's decay electron is also visible at the end of the track. While it is included in the display here, this delayed activity can be temporally separated at analysis time. (*Middle*) ν_e CC quasi-elastic event. (*Bottom*) NC resonant π^0 production, with a π^0 and proton in the final state. One decay photon carries the majority of the π^0's momentum, and its activity is clearly separated from the interaction point.

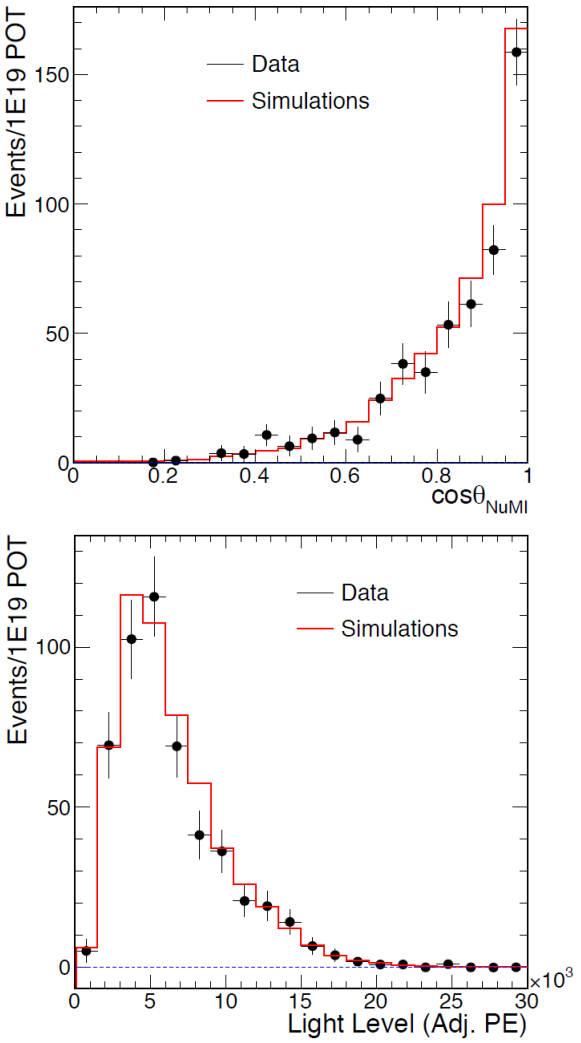

Figure 4: NuMI neutrino events in the NDOS, data and simulation. (*Top*) Reconstructed direction of the longest track relative to the nominal beam direction. (*Bottom*) Total observed energy in the event, shown here in units of "adjusted photoelectrons". Cosmic ray backgrounds, measured using beam-off data, have been subtracted from both distributions.

using NuMI neutrino events: the reconstructed primary track direction and the total visible energy. The data and simulation are in excellent agreement.

The NDOS continues to operate. FD construction has begun and will proceed over a two-year period ending Summer 2014. Neutrino data taking will commence with a partial detector (~5 kton) when the NuMI beam returns in May 2013. After a six-month beam commissioning period, the NuMI line will be ready for its full 700-kW operation. Figure 5 shows the expected NOvA exposure during early running.

4. $\nu_e / \bar{\nu}_e$ appearance

NOvA will begin its oscillation data run in ν mode, that is with the NuMI horn configured to focus positive secondary hadrons. While FD construction and NuMI commissioning will still be underway during the first year of data taking, NOvA can nonetheless reach a 5σ C.L. observation of θ_{13}-driven $\nu_\mu \rightarrow \nu_e$ oscillations after one year, assuming the normal mass hierarchy. Figure 6 shows how this sensitivity changes with time.

The baseline NOvA exposure is $3.6{\times}10^{21}$ protons-on-target (p.o.t.), which can be accumulated in six years at design intensities, with a 14-kton FD. For the sensitivities shown below, this exposure is assumed divided evenly between ν and $\bar{\nu}$ running, a split that works well for many parameter scenarios but is nonetheless adjustable. The analysis techniques used here are those described in the NOvA Technical Design Report [5]. Updated analyses for use in the first NOvA results are under active development.

Table 1 shows the number of ν_e and $\bar{\nu}_e$ CC event candidates expected after a six-year run. Since these counts

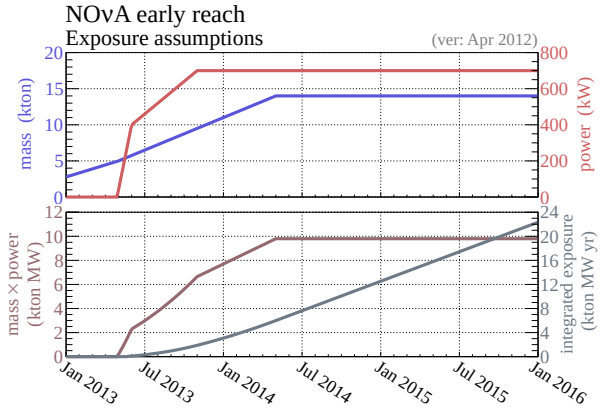

Figure 5: Expected development of detector mass, beam power, instantaneous exposure, and integrated exposure in the first few years of NOvA running.

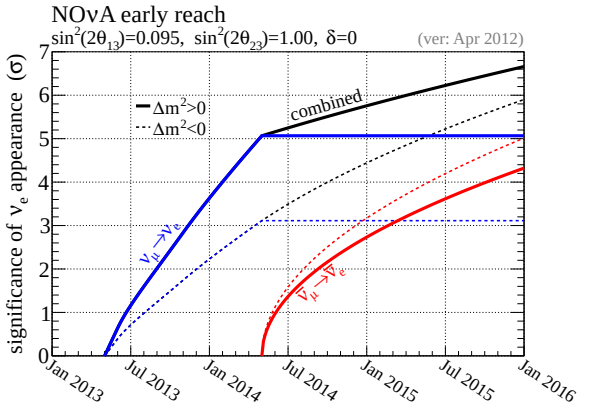

Figure 6: Sensitivity to $\nu_\mu \to \nu_e$ and $\overline{\nu}_\mu \to \overline{\nu}_e$ oscillations in early running. The solid (dashed) lines assume the normal (inverted) hierarchy. The red curves that begin May 2014 assume a switch to $\overline{\nu}$ running after one year. This run plan is merely an example, and the time of switching to $\overline{\nu}$ running is flexible. The black curves labeled "combined" show the appearance significance for the combined $\nu_\mu \to \nu_e$ and $\overline{\nu}_\mu \to \overline{\nu}_e$ samples.

depend strongly on the exact oscillation parameters, a sort of "average" is shown here by assuming no matter effects, no solar oscillations, and $\theta_{23}=\frac{\pi}{4}$. The signal efficiency is ~45% and the neutral current (NC) leakage rate is ~1%. These rates are somewhat higher than those in the Technical Design Report as the analysis cuts have been reoptimized for a non-zero value of θ_{13} [5].

Given its narrow-band beam, NOvA primarily measures oscillations of 2 GeV neutrinos. Thus, the appearance measurement approximately reduces to the extraction of two numbers from the data: the probabilities for $\nu_\mu \to \nu_e$ and $\overline{\nu}_\mu \to \overline{\nu}_e$ oscillations at 2 GeV. These two

	ν	$\overline{\nu}$
NC	19	10
ν_μ CC	5	<1
ν_e CC	8	5
total bg.	32	15
$\nu_\mu \to \nu_e$ CC	68	32

Table 1: Representative numbers of $\nu_\mu \to \nu_e$ and $\overline{\nu}_\mu \to \overline{\nu}_e$ candidate events expected in the FD after three years each of ν and $\overline{\nu}$ running, assuming $\sin^2(2\theta_{13})$=0.095. The two columns are labeled by running mode, ν or $\overline{\nu}$. Each row includes both right- and wrong-sign components.

probabilities depend on both the mass hierarchy and the value of the CP-violating phase δ, and it is instructive to see these dependencies graphically. Figure 7 shows the locus of possible values for these two probabilities for a given set of mixing angles. Overlayed on the figure are the expected 1σ and 2σ C.L. contours for a particular test point after six years of NOvA running. This representation of the appearance measurements, though approximate, makes plain the nature of NOvA's hierarchy and CP violation sensitivity. For example, no possible inverted hierarchy scenarios are included in the 2σ intervals for the test point shown, so the inverted hierarchy would be excluded by at least 2σ in this scenario.[2] Figure 7 also demonstrates that the significance with which NOvA can establish the hierarchy depends on δ. This significance is shown explicitly as a function of δ in Figure 8.

By the end of the primary NOvA run, the T2K experiment will have a significant $\nu_\mu \to \nu_e$ oscillation data set of its own, and the appearance probabilities for T2K depend relatively little on the mass hierarchy [6]. Thus, potential degeneracies in the NOvA measurement can be partially lifted by including T2K data. The combined sensitivity is shown in Figure 9.

The examples given so far have assumed $\sin^2(2\theta_{23}) = 1$. ν_μ disappearance measurements in the coming years, including those from NOvA (see below), will provide increased precision on $\sin^2(2\theta_{23})$, and it is possible that non-maximal mixing will be established. Figure 10 shows how non-maximal mixing

[2] A statistical note: the confidence levels shown in this figure assume one free parameter, with 2σ corresponding to $-2\Delta\log\mathcal{L} = 4$. This is appropriate given that the 2D space $\{P(\nu_e), P(\overline{\nu}_e)\}$ is not actually dense with possible answers. One can also read the contours as representing the $-2\Delta\log\mathcal{L}$ surface itself, allowing comparisons between the test point and any alternative allowed hypothesis. In either case, this figure is intended to provide an intuitive picture of the measurement principle, the sensitivity of which is quantified more transparently elsewhere.

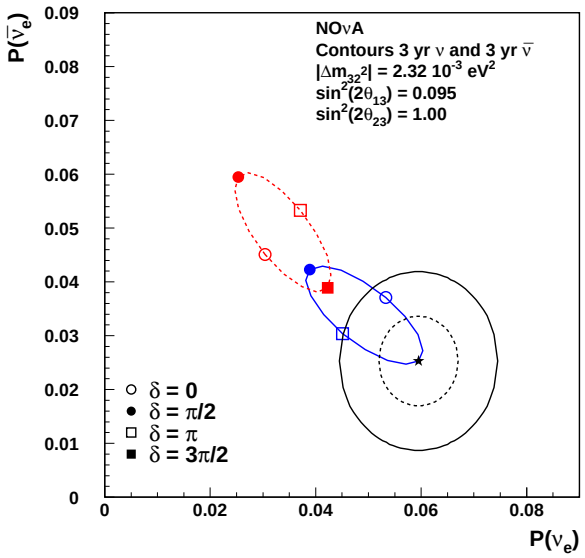

Figure 7: An overview of the NOvA appearance measurements. For $\sin^2(2\theta_{13}) = 0.095$ and $\sin^2(2\theta_{23}) = 1$, all possible values for the 2-GeV appearance probabilities $P(\nu_e)$ and $P(\bar{\nu}_e)$ are shown. The solid blue (dashed red) ellipse corresponds to the normal (inverted) hierarchy scenarios, with δ varying as one moves around each ellipse. 1σ and 2σ sensitivities to $P(\nu_e)$ and $P(\bar{\nu}_e)$ are shown in black for the test case at $\delta = \frac{3\pi}{2}$, normal hierarchy (starred point).

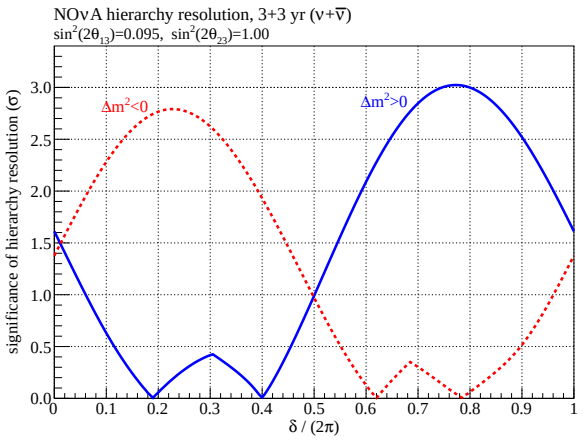

Figure 8: Significance with which NOvA can resolve the mass hierarchy as a function of δ for the indicated values of $\sin^2(2\theta_{13})$ and $\sin^2(2\theta_{23})$. 3.6×10^{21} p.o.t., evenly split between ν and $\bar{\nu}$ running, is assumed. The solid blue (dashed red) curve shows the expected significance assuming the normal (inverted) hierarchy.

influences the NOvA appearance measurements. In particular, the set of $\{P(\nu_e), P(\bar{\nu}_e)\}$ values that NOvA can measure at 2 GeV is now described by four ellipses rather than two, with the higher (lower) probability

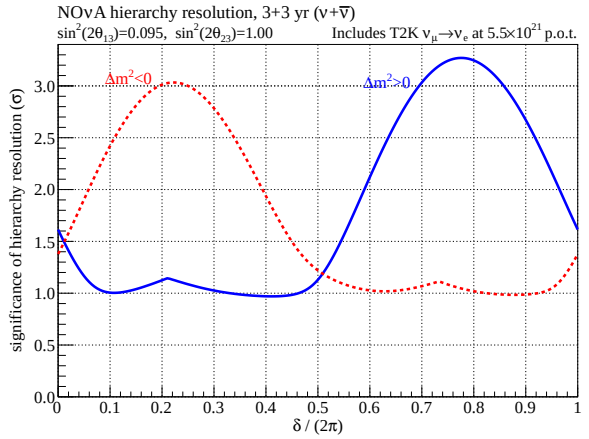

Figure 9: A version of Figure 8 that includes 5.5×10^{21} p.o.t. of T2K $\nu_\mu \rightarrow \nu_e$ data. The T2K data helps lift the degeneracy in unfavorable hierarchy/δ scenarios.

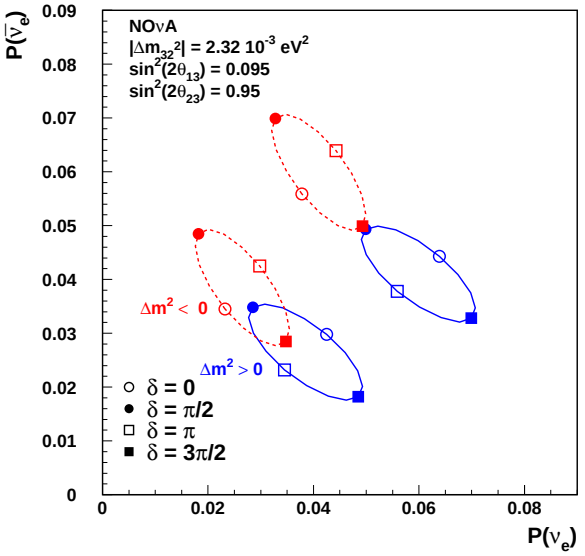

Figure 10: Similar to Figure 7 but with $\sin^2(2\theta_{23}) = 0.95$. The possible values for the appearance probabilities $P(\nu_e)$ and $P(\bar{\nu}_e)$ at 2 GeV have split, with the ellipses on the upper right (lower left) corresponding to $\theta_{23} > \frac{\pi}{4}$ ($\theta_{23} < \frac{\pi}{4}$).

cases corresponding to $\theta_{23} > \frac{\pi}{4}$ ($\theta_{23} < \frac{\pi}{4}$). Equivalently, the higher probability cases are those where the ν_3 state has more ν_μ than ν_τ admixture, and vice versa.

This bifurcation in the set of possible outcomes allows NOvA to make a measurement of this flavor balance (*i.e.*, of the θ_{23} octant). If $\sin^2(2\theta_{23}) < 1$, then, the NOvA appearance data will provide information on the mass hierarchy, δ, and the θ_{23} octant simultaneously.

Figure 11 shows NOvA's sensitivity to these three unknowns under two example scenarios, one in the degenerate regime and one not. Several features in the figure deserve mention. (1) The absence of any inverted hierarchy contours in the top panel indicates the $>2\sigma$ significance of hierarchy determination expected in this scenario. (2) The bottom panel shows a "degenerate" scenario, in which CP violation and long-baseline matter effects introduce cancelling perturbations in the oscillation probabilities. In such scenarios, NOvA provides only correlated information on the mass hierarchy and δ. (3) NOvA's θ_{23} octant sensitivity is largely independent of the hierarchy and δ. This is seen qualitatively in Figure 10 by the separation of the two octants' probabilities, and it is visible in the bottom panel here, where the correct octant is strongly preferred despite the presence of ambiguities in determining the mass hierarchy and δ.

4.1. Disappearance

While electron identification capability was key in the design of NOvA, the detectors also have excellent energy resolution for ν_μ charged current events, particularly for quasi-elastic interactions, and NOvA will make precision measurements of the atmospheric oscillation parameters $\sin^2(2\theta_{23})$ and $|\Delta m^2_{\rm atm}|$ through ν_μ and $\overline{\nu}_\mu$ disappearance. Like the appearance analyses, the disappearance analyses are under active development, and the sensitivities shown here come from earlier estimates [5] updated to include the latest knowledge of beam and detector performance.

NOvA's narrow-band 2-GeV spectrum and matching 810-km baseline mean that the ν_μ flux is largely oscillated away at the FD. Figure 12 shows the expected reconstructed energy spectrum for ν_μ and $\overline{\nu}_\mu$ CC quasi-elastic events after three years each of ν and $\overline{\nu}$ running at design exposures. Both a maximal and a non-maximal mixing scenario are shown, and these are readily distinguished given the expected event counts and the energy resolution of 4% assumed for this quasi-elastic sample.

Figure 13 shows the sensitivity to $\sin^2(2\theta_{23})$ and $|\Delta m^2_{\rm atm}|$ for three test cases. If $\sin^2(2\theta_{23})$ is near the current global best-fit value of 0.95 [7], NOvA can establish non-maximal mixing at $>2\sigma$.

5. Closing

NOvA FD construction is underway at Ash River, and ND cavern excavation is now beginning at Fermilab. The ND-sized prototype detector, NDOS, has operated for two years at Fermilab and has allowed rapid development of assembly procedures and analysis tools.

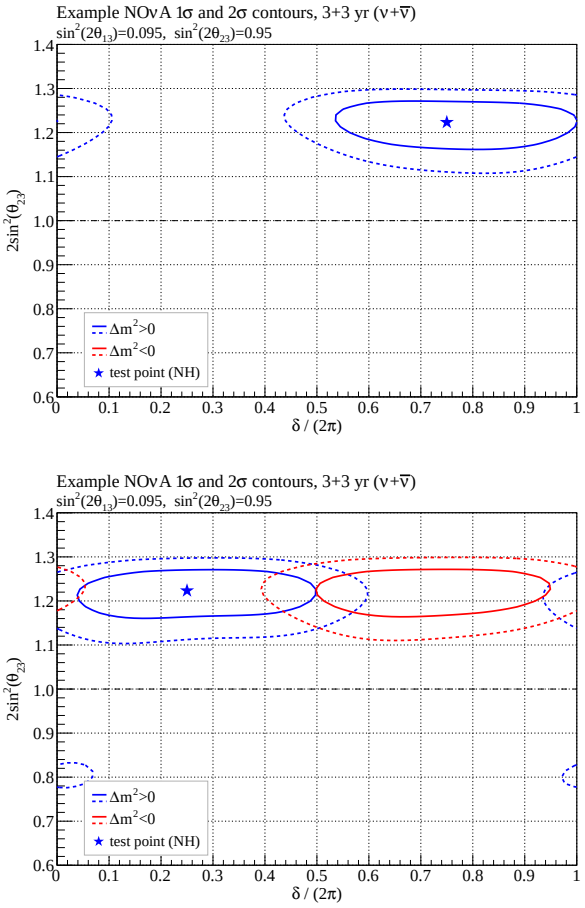

Figure 11: Example 1σ and 2σ allowed regions for δ and $2\sin^2(\theta_{23})$ for the two starred test points. (*Top*) Test point at $\sin^2(2\theta_{13}) = 0.095$, $\sin^2(2\theta_{23}) = 0.95$, $\theta_{23} > \frac{\pi}{4}$, $\delta = \frac{3\pi}{2}$, normal hierarchy (NH). (*Bottom*) Same except for $\delta = \frac{\pi}{2}$. The blue (red) contours show the expected allowed ranges under a normal (inverted) hierarchy assumption, and the confidence levels are established assuming two free parameters.

The NuMI beam will return May 2013, and NOvA will begin collecting neutrino data immediately with a partial detector. Full instantaneous exposure will be reached in summer 2014 when the 14-kton FD is complete. With a six-year run, NOvA can unambiguously resolve the neutrino mass hierarchy at >95% C.L. for over a third of possible values of δ. NOvA will otherwise provide δ-dependent hierarchy determination plus measurements of θ_{13}, θ_{23}, $|\Delta m^2_{\rm atm}|$, and δ itself.

NOvA will begin its FD neutrino run in ν mode, with a future switch to $\overline{\nu}$ running yet to be scheduled. For the normal mass hierarchy, NOvA can achieve 5σ C.L. observation of atmospheric-regime $\nu_\mu \rightarrow \nu_e$ oscillations with its first year of data, even with the exposure limita-

tions of on-going detector construction and NuMI beam commissioning.

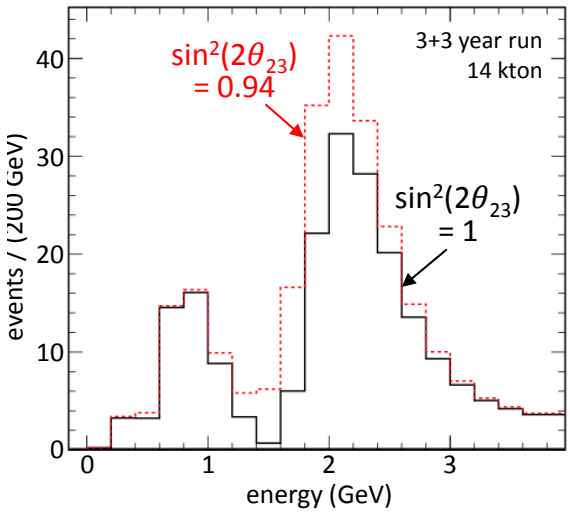

Figure 12: Reconstructed neutrino energy spectrum expected at the FD in two scenarios after a 3+3 year (ν+$\overline{\nu}$) run. The solid black (dashed red) histogram is for $\sin^2(2\theta_{23}) = 1$ ($\sin^2(2\theta_{23}) = 0.94$).

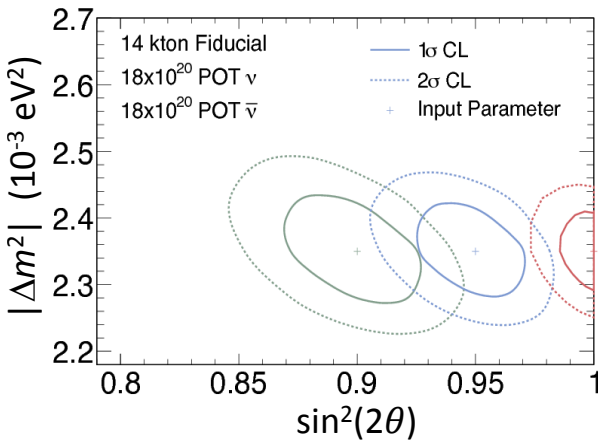

Figure 13: NOvA 1σ and 2σ sensitivity to $\sin^2(2\theta_{23})$ and $|\Delta m^2_{\text{atm}}|$ after a 3+3 year (ν+$\overline{\nu}$) run.

Acknowledgments

The author acknowledges support from the Department of Energy under contracts ER40701 and ER41735.

References

[1] Y. Abe *et al.*, Phys. Rev. Lett. **108**, 131801 (2012); Y. Abe *et al.*, arXiv:1207.6632 (2012).
[2] F. P. An *et al.*, Phys. Rev. Lett. **108**, 171803 (2012); See also the update in these proceedings (D. Dwyer).
[3] J. K. Ahn *et al.*, Phys. Rev. Lett. **108**, 191802 (2012).
[4] K. Anderson *et al.*, FERMILAB-DESIGN-1998-01 (1998).
[5] D. S. Ayres *et al.*, FERMILAB-DESIGN-2007-01 (2007).
[6] K. Abe *et al.*, Phys. Rev. Lett. **107** (2011) 041801; See also the update in these proceedings (T. Nakaya).
[7] G. L. Fogli *et al.*, Phys. Rev. D **86**, 013012 (2012).